Twirling Elastica: Kinks, Viscous Drag, and Torsional Stress

Stephan A. Koehler[1] and Thomas R. Powers[2]

[1]*Division of Engineering and Applied Sciences, Harvard University, Cambridge, Massaschusetts 02138*
[2]*Division of Engineering, Brown University, Providence, Rhode Island 02912*

(Received 6 April 2000)

Biological filaments such as DNA or bacterial flagella are typically curved in their natural states. To elucidate the interplay of viscous drag, twisting, and bending in the overdamped dynamics of such filaments, we compute the steady-state torsional stress and shape of a rotating rod with a kink. Drag deforms the rod, ultimately extending or folding it depending on the kink angle. For certain kink angles and kink locations, both states are possible at high rotation rates. The agreement between our macroscopic experiments and the theory is good, with no adjustable parameters.

PACS numbers: 87.16.–b, 05.45.–a, 46.70.Hg, 47.15.Gf

The coupling of viscous stresses from fluid flow to deformations of elastic fibers is important in many situations, such as paper manufacture, flexible microstructures in microelectromechanical systems devices, and the dynamics of flexible biological filaments. The last example includes spinning filaments, such as bacterial flagella, DNA, and supercoiling colonies of mutant strains of *Bacillus subtilis.* The rotary motors of *E. coli* rotate the flagellar bundle up to 9000 rpm [1]. In DNA transcription, if rotational motion of the RNA polymerase is blocked, then the DNA twirls at typical rates of 300–600 rpm as it is pulled through the enzyme [2]. Finally, the mutant *B. subtilis* cells fail to separate as they divide, and form long fibers which rotate as they grow [3].

Although these filaments are often modeled as intrinsically straight elastic rods, natural bends can have significant effects. For example, natural curvature in bacterial flagella is crucial for generating thrust; mutants with straight flagella cannot swim [4]. Proteins can bind to DNA and impose sharp, large-angle bends [5], which can greatly enhance the torsional stress due to viscous drag during transcription. Similar torsional stresses from intrinsic bends have been estimated to be large enough to affect gene activity or DNA structure even in the absence of external anchoring [6]. As we shall recall below, kinks generically *trap* torsional stress in specific regions of a rotating filament. Finally, there is evidence that intrinsic bends may arise at the hairpin loops during the formation of supercoiled colonies of *B. subtilis* [7].

To gain intuition on how sharp intrinsic bends affect shape and twist in the overdamped (inertialess) regime of cellular motions, we study a bent elastic rod rotating in an extremely viscous fluid, and ask, how do the shape and torsional stress depend on the twirling rate? For simplicity we disregard Brownian effects. We first describe how rotation affects the shape, then we formulate and solve the problem using slender-body theory, and finally we compare our predictions with experimental results.

The shape and stresses of a rotating elastic rod in a viscous fluid depend on its stress-free state. At low rotation rates, a naturally straight rod twirled about its long axis (which is along the z axis, say) remains straight, but twists and spins about z. At higher rates this state is unstable, the centerline writhes and slowly rotates about z, and each element of the rod rapidly spins about the local tangent. This motion is a hybrid of crankshaft and speedometer-cable motion [8].

A naturally bent rod rotating in a viscous fluid behaves very differently. Consider a rod made of two straight legs joined at a right angle. Align one leg along the vertical (z) axis and twirl it with velocity $\omega\hat{\mathbf{z}}$. Unlike the naturally straight rod, the centerline of this rod will distort from its unstressed state for *any* rotation rate, since the free leg experiences translational drag. This translational drag will wrap the free leg around z (insets, Figs. 1 and 2), and twist the held leg. In comparison to the naturally straight rod, the torsional stress in the held leg is very large, for a given ω.

Viscous stresses tend to straighten out a rod with a right-angle kink (Fig. 1). To see why, it is convenient to work in the frame of the twirling rod, with an unperturbed fluid velocity $\mathbf{v} = \omega\hat{\mathbf{z}} \times \mathbf{r}$, where $\mathbf{r} = \mathbf{r}(s, t)$ is the position of the rod at time t, and s is arclength. Suppose the free leg aligns parallel to the x axis for $\omega = 0$; i.e., the "L" lies in the z-x plane. For small ω ("small" will be defined below), translational drag deflects the free leg in the y direction, which causes the held leg to bend away from the rotation axis in the y direction. Thus the held leg lies in a region where the flow is in the $-x$ direction; this flow deflects the held leg, rotating the joint to extend the rod. For small ω, the sense of the joint rotation is *independent* of the exterior kink angle, α. As ω increases, rods with small to moderate α (L-shaped) will extend, whereas rods with large α (V-shaped) will fold.

These arguments suggest there should be a critical angle dividing the ultimate (large ω) extending and folding behaviors, but further reflection reveals that both states are possible at large rotation rates. Imagine that a rod with a right-angle kink is bent by an external force that brings the two legs together so the rod looks like a "U" with a sharp kink. Sufficient rotational flow will cause folding for the same reason the V-shaped rod eventually folds. At high rotation rates, the viscous stresses will be large

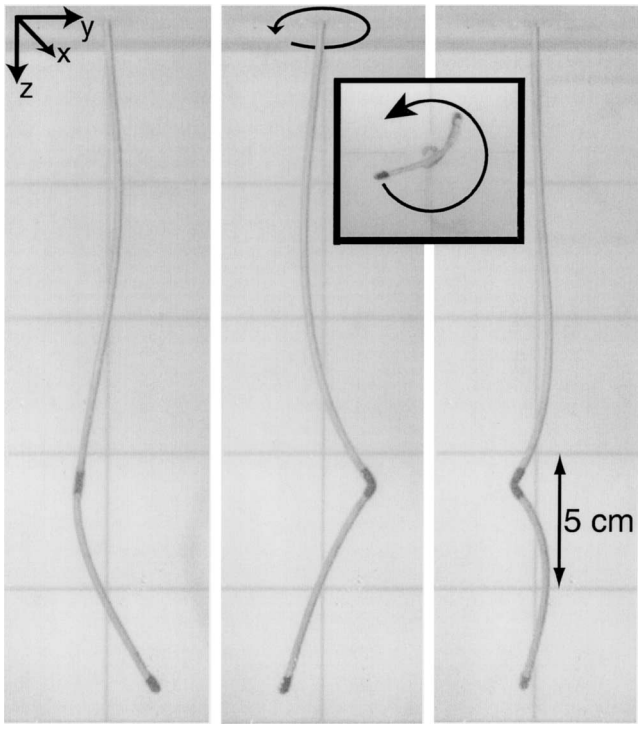

FIG. 1. Time sequence, from left to right, showing the steady-state shape of a naturally L-shaped rod twirling in glycerol. A motor (above, not shown) rotates the rod at 200 rpm. Gravity is along z, and x points into the page. The container is a Plexiglas box 31 cm $\times$ 31 cm wide and 28 cm tall. Inset is the view from below, in which the rod rotation is counterclockwise.

enough to hold the rod in this folded state even when the external force is released. Thus, we expect bistability at large rotation rates: Figs. 1 and 2 show the same rod and same rotation rate with different initial conditions. These steady-state shapes are stable against small-amplitude perturbations, but sufficiently large perturbations lead to a transition from extended to folded and vice versa.

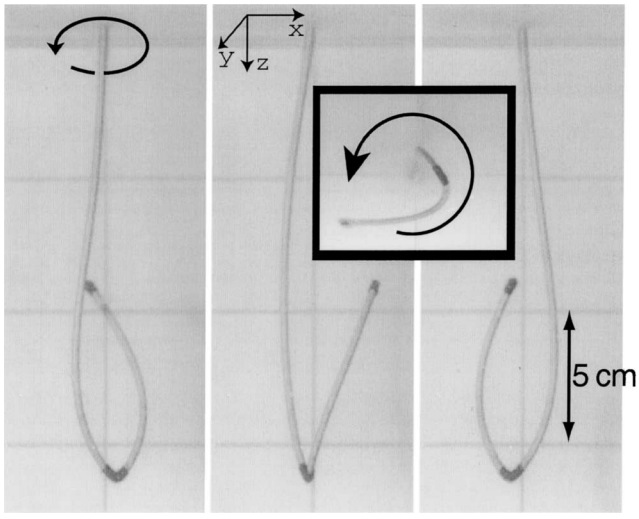

FIG. 2. Bistability at sufficiently high ω. The same rod as in Fig. 1, spinning at 200 rpm, but a different state, obtained by bending the rod upwards into a V-shape at the onset of twirling. Inset: view from below.

We now turn to the mathematical analysis. For a slender rod (radius a much less than length L), deformations can be described by the configuration of an orthonormal material frame $\{\hat{\mathbf{e}}_1, \hat{\mathbf{e}}_2, \hat{\mathbf{e}}_3\}$ embedded in the rod [9], with $\hat{\mathbf{e}}_3 = \partial \mathbf{r}/\partial s \equiv \mathbf{r}_s$. The rates of rotation of this frame with respect to arclength and time define the angular strain $\boldsymbol{\Omega}$ and velocity $\boldsymbol{\omega}$:

$$(\hat{\mathbf{e}}_i)_s = \boldsymbol{\Omega} \times \hat{\mathbf{e}}_i, \qquad (\hat{\mathbf{e}}_i)_t = \boldsymbol{\omega} \times \hat{\mathbf{e}}_i, \tag{1}$$

with $i = 1$–3. Associated with these strains are internal elastic stresses, which give rise to a force $\mathbf{F}(s)$ and a moment $\mathbf{M}(s)$ acting on the cross section at s. For an isotropic linearly elastic rod, the constitutive relation is $\mathbf{M} = A\mathbf{r}_s \times \mathbf{r}_{ss} + C\mathbf{r}_s\mathbf{r}_s \cdot \boldsymbol{\Omega}$, where A is the bending stiffness and C is the twisting stiffness [9]. Note $\mathbf{M} = A\boldsymbol{\Omega}$ when $\Gamma \equiv C/A = 1$. In the (overdamped) limit of zero Reynolds number Re, the elastic force and moment per unit length balance exactly with the viscous drag force and moment per unit length:

$$\mathbf{F}_s - \mathbf{f} = \mathbf{0}, \tag{2}$$

$$\mathbf{M}_s + \mathbf{r}_s \times \mathbf{F} - \mathbf{m} = \mathbf{0}. \tag{3}$$

From slender-body hydrodynamics [10], the leading-order drag force and moment per unit length are

$$\mathbf{f} = \zeta_\parallel \mathbf{r}_s\mathbf{r}_s \cdot \mathbf{r}_t + \zeta_\perp(\mathbf{r}_t - \mathbf{r}_s\mathbf{r}_s \cdot \mathbf{r}_t), \tag{4}$$

$$\mathbf{m} = \zeta_r \mathbf{r}_s\mathbf{r}_s \cdot \boldsymbol{\omega}, \tag{5}$$

where $\zeta_\perp \approx 2\zeta_\parallel \approx 4\pi\eta/[\log(L/2a) + c]$ (η is viscosity, c is a constant of order unity) and $\zeta_r \approx 4\pi\eta a^2$ [10]. Although the slender-body approximation is invalid near the kink where the curvature diverges, it does have the correct (linear) ω dependence for the translational drag per unit length, and will therefore give the correct (nonlinear) scaling of the shape and torsional stress with ω.

As emphasized in Ref. [6], kinks block speedometer-cable motion, since sharp curvature implies a large elastic energy cost for rotation about the local tangent. Thus we consider pure crankshaft motion of the centerline about the axis of rotation. Furthermore, the torsional stress $C\mathbf{r}_s \cdot \boldsymbol{\Omega}$ due to rotational drag of the held leg is $\mathcal{O}(\zeta_r \omega L)$, much smaller than the torsional stress due to *translational* drag of the free leg, which for small ω is $\mathcal{O}(\zeta_\perp \omega L^3)$. As we shall verify below, the twist due to translation dominates that due to rotation even at large ω, as long as L/a is sufficiently large. Hence we set $\zeta_r = 0$ for further simplicity. Finally, we take the kink angle α to be clamped at a value independent of ω.

We desire the steady-state solution to (1)–(5) for $\mathbf{r}_t = \boldsymbol{\omega} \times \mathbf{r}$, with $\boldsymbol{\omega} = \omega\hat{\mathbf{z}}$; as our experiments confirm there is no oscillatory behavior as expected at the low Reynolds number. Fifteen boundary conditions at the ends are required for the fifteen unknowns: $\mathbf{r}, \mathbf{r}_s, \hat{\mathbf{e}}_1$ ($\hat{\mathbf{e}}_2 = \mathbf{r}_s \times \hat{\mathbf{e}}_1$), $\mathbf{M}$, and $\mathbf{F}$. Taking the x and y axes to rotate about z with rate ω, we demand $\mathbf{r}(0) = \mathbf{0}$, $\mathbf{r}_s(0) = \hat{\mathbf{z}}$, and $\hat{\mathbf{e}}_1(0) = \hat{\mathbf{x}}$ at the held end. The free end experiences no force and moment: $\mathbf{F}(L) = \mathbf{0}$ and $\mathbf{M}(L) = \mathbf{0}$. Finally, fifteen

conditions must be enforced at the position of the joint, $s = L_1$. These conditions are the continuity of position, force, and moment, and $\mathbf{r}_s(L_1^+) = \mathbf{r}_s(L_1^-)\cos\alpha + \hat{\mathbf{e}}_1 \times (L_1^-)\sin\alpha$, and $\hat{\mathbf{e}}_1(L_1^+) = -\mathbf{r}_s(L_1^-)\sin\alpha + \hat{\mathbf{e}}_1(L_1^-)\cos\alpha$. The twist is discontinuous across the kink, since the twisting moment on one side can balance with a bending moment on the other; kinks trap torsional stress.

We measure length in units of L, time in units of the bending relaxation time $\zeta_\perp L^4/A$, force in units of A/L^2, and moment in units of A/L. The shape of the rod is then controlled by the dimensionless rotation rate $\chi = \zeta_\perp \omega L^4/A$ (cf. [11]) and the geometrical quantities α and L_1/L. In our macroscopic experiments of Figs. 1 and 2, the rod is a steel compression spring wrapped in Teflon™ tape, immersed in glycerol, with $\eta \approx 20.0$ erg sec/cm^3, $L = 29$ cm, $a = 0.16$ cm, $\alpha \approx 87°$, and $A \approx C \approx 2.2 \times 10^5$ dyne cm^2. For our motor speeds of 5–500 rpm, χ ranges from 55–5500.

For small χ the shape and stress can be obtained to linear order in χ. For the linear calculation only, it is convenient to write (1)–(5) in terms of $\mathbf{r}$ and set $\zeta_\perp = \zeta_\parallel$; in fact, $\zeta_\parallel$ will not enter the linear calculation. The constitutive relation, the moment balance equation (3) (which now has $\mathbf{m} = \mathbf{0}$), and $\mathbf{r}_s \cdot \mathbf{r}_s = 1$ imply $\mathbf{F} = -\mathbf{r}_{sss} + \Gamma\Omega\mathbf{r}_s \times \mathbf{r}_{ss} + \Lambda\mathbf{r}_s$, where $\Omega = \mathbf{r}_s \cdot \mathbf{\Omega}$, and Λ is the unknown part of $\mathbf{r}_s \cdot \mathbf{F}$. Force balance is thus

$$\chi\hat{\mathbf{z}} \times \mathbf{r} = -\mathbf{r}_{ssss} + \Gamma\Omega\mathbf{r}_s \times \mathbf{r}_{sss} + (\Lambda\mathbf{r}_s)_s . \quad (6)$$

Since $\zeta_r = 0$, the tangential moment balance (3) implies $\Omega_s = 0$, i.e., constant twist in each leg.

For simplicity, consider a right-angle kink, $\alpha = \pi/2$. If $\chi = 0$, then $\Omega = \Lambda = 0$, and the rod is undeformed. To first order in χ, the deformation of both legs of the rod is evidently along the y direction; therefore,

$$\mathbf{r}(s) \approx \begin{cases} s\hat{\mathbf{z}} + y(s)\hat{\mathbf{y}} & 0 \le s \le L_1 , \\ L_1\hat{\mathbf{z}} + (s - L_1)\hat{\mathbf{x}} + y(s)\hat{\mathbf{y}} & L_1 \le s \le 1 . \end{cases} \quad (7)$$

Force balance implies that $\Lambda_s = 0$ in both legs, $y_{ssss} = 0$ for $0 \le s \le L_1$, and $\chi(s - L_1) = -y_{ssss}$ for $L_1 \le s \le 1$. The boundary conditions at the ends of the rod are $y(0) = y_s(0) = 0$, and $y_{ss}(1) = y_{sss}(1) = \Omega(1) = \Lambda(1) = 0$. Therefore, $\Lambda = \Omega = 0$ for $L_1 < s \le 1$; note that the twist for $0 \le s < L_1$ is *not* zero: the kink has trapped the twist. Continuity requires $y(L_1^-) = y(L_1^+)$; also,

$$\begin{aligned} \hat{\mathbf{e}}_1^- &= \hat{\mathbf{x}} + \Gamma\Omega L_1\hat{\mathbf{y}} , & \hat{\mathbf{e}}_1^+ &= -\hat{\mathbf{z}} - y_s^+\hat{\mathbf{y}} , \\ \hat{\mathbf{e}}_2^- &= \hat{\mathbf{y}} - \Gamma\Omega L_1\hat{\mathbf{x}} , \quad \text{and} & \hat{\mathbf{e}}_2^+ &= \hat{\mathbf{y}} - y_s^+\hat{\mathbf{x}} + y_s^-\hat{\mathbf{z}} , \\ \hat{\mathbf{e}}_3^- &= \hat{\mathbf{z}} + y_s^-\hat{\mathbf{y}} , & \hat{\mathbf{e}}_3^+ &= -\hat{\mathbf{x}} + y_s^+\hat{\mathbf{y}} , \end{aligned} \quad (8)$$

where $\hat{\mathbf{e}}_i^\pm = \hat{\mathbf{e}}_i(L_1^\pm)$, etc. Using (8), the condition on the jump in the material frame becomes $\Gamma\Omega L_1 = y_s^+$, continuity of force becomes $y_{sss}^- = y_{sss}^+$ and $\Lambda^- = 0$, and continuity of moment becomes $y_{ss}^- = 0$ and $\Gamma\Omega = y_{ss}^+$. Thus we find a (dimensional) twist stress of $C\Omega = -\zeta_\perp\omega(L - L_1)^3/3$ in the held leg. The (dimensional) shape of the rod is given by

$$y(s) = -\frac{\zeta_\perp\omega}{12A}\, s^2(3L_1 - s)\,(L_1 - L)^2, \qquad s \le L_1 , \quad (9)$$

and

$$y(s) = \frac{\zeta_\perp\omega}{A}\left[\left(\frac{L_1^2L^3}{6} - \frac{3L_1^3L^2}{4} + L_1^4L - \frac{49L_1^5}{120}\right) + L_1^2 s\left(\frac{L^2}{4} - \frac{L_1L}{2} + \frac{5L_1^2}{24}\right) + s^2L^2\left(\frac{L_1}{4} - \frac{L}{6}\right) + s^3L\left(\frac{L}{12} - \frac{L_1}{6}\right) + \frac{s^4L_1}{24} - \frac{s^5}{120}\right], \qquad s \ge L_1 . \quad (10)$$

To solve for the shape and stress when χ is not small, we must use numerical methods. However, we can obtain the χ dependence of the various quantities for $\chi \gg 1$ using a simple argument. Since the rod is mostly aligned along the z axis at high twirling rates (in both the folding and extending cases), $\mathbf{r} = \hat{\mathbf{z}}s + \mathbf{r}_\perp$ with $|\mathbf{r}_\perp| \to 0$ as $\chi \to 0$. Ignoring the terms involving Λ, and all numerical prefactors, (6) reduces to

$$\hat{\mathbf{z}} \times \mathbf{r}_\perp = -\frac{1}{\chi}\,\mathbf{r}_{\perp ssss} + \frac{\Omega}{\chi}\,\hat{\mathbf{z}} \times \mathbf{r}_{\perp sss} + \ldots . \quad (11)$$

The curvature and $|\mathbf{r}_\perp|$ are very small except in a boundary layer near the kink at $s = L_1$; rescaling $s - L_1 = (\bar{s} - L_1)/\chi^{1/4}$, we find that the translational drag, bending, and twisting forces per length all balance for large χ if $\Omega \propto \chi^{1/4}$. On the other hand, we can balance the moment $C\Omega$ against the approximate translational drag $\int ds\,(\zeta_\perp\omega|\mathbf{r}_\perp|)\,|\mathbf{r}_\perp|$ to find $|\mathbf{r}_\perp| \propto \chi^{-1/4}$. This change in shape with χ implies that the *effective* rotational friction coefficient $\zeta_{r,\mathrm{eff}} \equiv C\Omega/\omega$ decreases as $\chi^{-3/4}$ for large χ.

Equations (1)–(5) are in standard form for the relaxation method [12]. The interval $0 \le s \le 1$ is replaced by a fine mesh, with two mesh points corresponding to $s = 1/2^\pm$. There is no need to introduce the intermediate tension variable Λ, which enforces fixed length, since (1) and the boundary condition on $\mathbf{r}_s$ at $s = 0$ imply $\mathbf{r}_s \cdot \mathbf{r}_s = 1$. For simplicity, we choose $\Gamma = 1$ and $\zeta_\parallel = \zeta_\perp/2$.

Figure 3 shows the total extension and torsional stress as functions of the twirling rate for a rod with $\alpha = 87°$ and $L_1/L = 2/3$ (as in Figs. 1 and 2). As χ increases, the initially L-shaped rod distorts and extends. At sufficiently large χ, a new branch of solutions appears which corresponds to folding. The situation is reminiscent of an imperfect bifurcation. To make the comparison with experiment, we have included a net downward force per unit length due

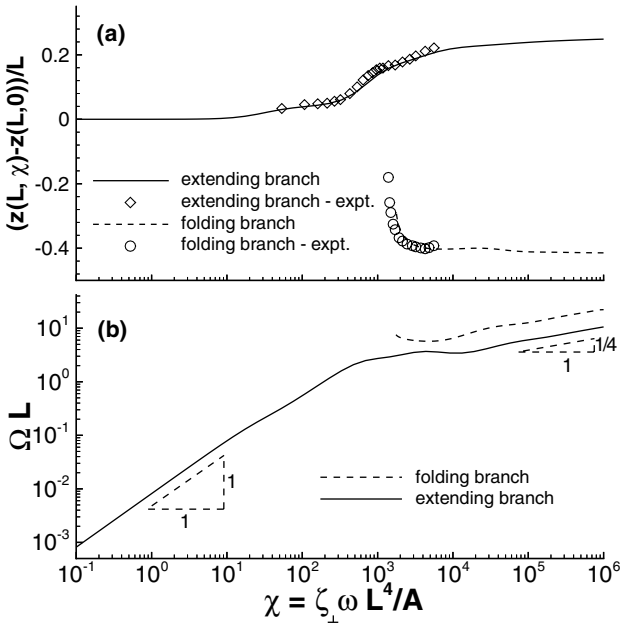

FIG. 3. (a) Theoretical predictions and experimental results for relative z displacement of rod free end ($s = L$) versus dimensionless rotation rate χ. (b) Theoretical prediction for dimensionless twist in the held leg versus χ. Note the agreement with the scaling arguments for Ω. $\alpha \approx 87°$; $L_1/L = \frac{2}{3}$.

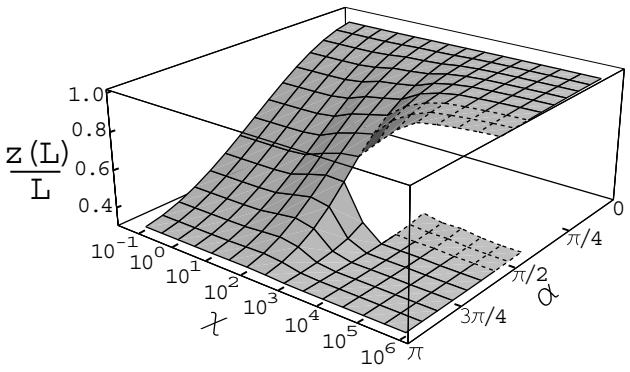

FIG. 4. Phase diagram for twirling a rod with a kink at $L_1 = \frac{2}{3}L$ (no gravity). For $\chi \gtrsim 1500$ and α near $\pi/2$, the rod is bistable, as indicated by the dashed lines. Here, $z = 1$ is fully extended and $z = \frac{1}{3}$ is completely folded.

to gravity (the filament's linear density is 0.167 g/cm and glycerol has a density around $\rho = 1.3$ g/cm^3). There is no fitting in Fig. 3. The agreement between theory and experiment is excellent. We expect the slender-body hydrodynamics approximations to work well since the curvature is gentle away from the small region near the kink (Figs. 1 and 2), and the two legs of the rod are separated by many rod radii even in the folded state (inset of Fig. 2). The Reynolds number $\mathrm{Re} \approx \omega r_{\max} a \rho/\eta$ is about 0.2 for ω around 500 rpm ($r_{\max}$ is the maximum transverse displacement of the rod, $\omega r_{\max}$ sets the velocity scale, and the rod *radius* a sets the length scale of the disturbance flow). Figure 3 also gives the dependence of the torsional stress on χ, confirming our scaling arguments that $\Omega \propto \chi$ for $\chi \ll 1$ and $\Omega \propto \chi^{1/4}$ for $\chi \gg 1$. We can now assess our neglect of ζ_r at large χ: demanding $(\zeta_r \omega L)/(\int ds\, \zeta_\perp \omega |\mathbf{r}_\perp|^2) \ll 1$ amounts to requiring $\chi^{3/4}(a/L)^2 \ll 1$, which is easily fulfilled for $L/a \approx 10^3$. Note that (within the slender-body hydrodynamics approximation) the twist has the $\chi^{1/4}$ dependence for both the folding and extending branches.

Figure 4 displays the "phase diagram" for a twirling bent rod. Rods with large kink angles (V-shaped) fold up as χ increases from zero, whereas rods with small kink angles extend. For intermediate kink angles, both states are possible at high χ; there is no critical angle dividing extending and folding. This behavior is generic as long as L_1/L is not too close to 0 or 1.

In conclusion, we have shown how kinks affect the deformation and torsional stress of a twirling elastic rod in a viscous fluid. Despite the linearity of the elastic constitutive relations (which derive from Hooke's law) and the equations for viscous flow (Stokes equations), we find nonlinear dependences on rotation rate at high rates due to the change in shape. Bacterial flagella, DNA, and fibers of *B. subtilis* are sufficiently flexible that typical rotation rates can cause the extending and folding studied here, which could be revealed using micromanipulation. An important extension of our work which would be relevant to DNA would be to carry out Brownian dynamics simulations of a rotating flexible rod with many kinks, as envisioned in Ref. [6].

We thank P. Nelson for posing the question that led to this work, and R. Goldstein, T. Peacock, H. Stone, C. Wiggins, and C. Wolgemuth for discussions. We thank H. Stone for partial support through the Harvard MRSEC and the Army Research Office Grant No. DAA655-97-1-014.

[1] B. Alberts, D. Bray, J. Lewis, M. Raff, K. Roberts, and J. D. Watson, *The Molecular Biology of the Cell* (Garland Publishing, Inc., New York, 1994), 3rd ed.
[2] R. A. Ikeda and C. C. Richardson, J. Biol. Chem. **262**, 3790 (1987).
[3] N. H. Mendelson, Proc. Natl. Acad. Sci. U.S.A. **73**, 1740 (1976).
[4] R. M. Macnab and M. K. Ornston, J. Mol. Biol. **112**, 1 (1977).
[5] See, e.g., J. L. Kim, D. B. Nikolov, and S. K. Burley, Nature (London) **365**, 512 (1993); **365**, 520 (1993).
[6] P. Nelson, Proc. Natl. Acad. Sci. U.S.A. **96**, 14 342 (1999).
[7] N. H. Mendelson (private communication).
[8] C. W. Wolgemuth, T. R. Powers, and R. E. Goldstein, Phys. Rev. Lett. **84**, 1623 (2000).
[9] A. E. H. Love, *A Treatise on the Mathematical Theory of Elasticity* (Dover Publications, New York, 1944), 4th ed.
[10] J. Keller and S. Rubinow, J. Fluid Mech. **44**, 705 (1976).
[11] C. H. Wiggins, D. Riveline, R. E. Goldstein, and A. Ott, Biophys. J. **74**, 1043 (1998).
[12] W. H. Press, W. T. Vetterling, S. A. Teukolsky, and B. P. Flannery, *Numerical Recipes in C* (Cambridge University Press, Cambridge, England, 1992), 2nd ed.